J Fluoresc (2012) 22:771–778
DOI 10.1007/s10895-011-1012-2

ORIGINAL PAPER

Interaction of CdTe Quantum Dots with 2,2-Diphenyl-1-Picrylhydrazyl Free Radical: A Spectroscopic, Fluorimetric and Kinetic Study

Oluwasesan Adegoke · Wadzanai Chidawanyika · Tebello Nyokong

Received: 15 July 2011 / Accepted: 20 October 2011 / Published online: 5 November 2011

Abstract The interaction of 2,2-diphenyl-1-picrylhydrazyl (DPPH$^{\bullet}$) free radical with thiol-capped CdTe quantum dots (QDs) has been studied by UV–vis spectroscopy, steady state and time resolved fluorescence measurements. Addition of DPPH$^{\bullet}$ radical to CdTe QDs resulted in fluorescence quenching. The interaction occurs through static quenching as this was confirmed by fluorescence lifetime measurements. Time course absorption studies indicates that DPPH$^{\bullet}$ may be reduced by interaction with QDs to the substituted hydrazine form (2,2-diphenyl-1-picrylhydrazine) DPPH-H. The mechanism of fluorescence quenching of CdTe QDs by DPPH$^{\bullet}$ is proposed.

Keywords 2,2-Diphenyl-1-picrylhydrazine · Fluorescence quenching · Quantum dots · Thioglycolic acid

Introduction

Colloidal semiconductor nanocrystal quantum dots (QDs) have attracted great interest in recent years due to their size-dependent properties. They exhibit tunable and intense fluorescence spectra [1–5], broad excitation spectra and favourable photostability [6–9]. Imaging and sensing applications have been proposed for QDs [7, 10–12].

The controlled fluorescence quenching of QDs such as cadmium telluride, cadmium selenide and cadmium sulfide, has led to the development of probes for sensing of a variety of molecules such as lysozome, deoxyribonucleic acid (DNA), anions, nitric oxide and copper ions [13–17]. Fluorescence quenching mechanisms of QDs have been studied in the presence of quenchers such as metal ions [8], nitroxyl radicals [18], vitamin B6 [19], and cardiolipin [20] as a basis for useful insight in developing fluorescence-based probes with great promise as substitutes for organic fluorescent dyes.

To date, only a few research studies have been focused on the interaction of stable free radicals with functionalized QDs. Radicals such as 4–amino-2,2,6,6-tetramethylpiperidine oxide (4-amino-TEMPO) have been reported to quench the fluorescence of CdSe QDs. Electron paramagnetic resonance (EPR) data suggested the strong binding of the radical to the QD surface while the nonlinear Stern-Volmer plot was a reflection of the accessibility of the QD to one or two 4-amino-TEMPO molecules [19]. 2,2-Diphenyl-1-picrylhydrazyl free radical (DPPH$^{\bullet}$, Scheme 1) which is a stable paramagnetic free radical with an intense purple colour, has historically been used as a primary spin-concentration standard in EPR. It is popularly known to be a good abstractor of hydrogen yielding its reduced counterpart 2,2-diphenyl-1-picrylhydrazine (DPPH-H) [21].

To the best of our knowledge, detailed interaction of thiol-capped CdTe quantum dots with DPPH$^{\bullet}$ have not been studied before the current manuscript. In this work, we report that the fluorescence of thioglycolic acid (TGA) capped CdTe QDs can be efficiently quenched by DPPH$^{\bullet}$ at different concentrations. The quenching mechanism of the TGA-capped CdTe by DPPH$^{\bullet}$, kinetics and influences of pH are investigated by combined steady state and time resolved fluorescence measurements. These results provide new fundamental insights into the process of fluorescence quenching of QDs by free radicals for development of

O. Adegoke · W. Chidawanyika · T. Nyokong (✉)
Department of Chemistry, Rhodes University,
Grahamstown 6140, South Africa
e-mail: t.nyokong@ru.ac.za

Scheme 1 The structure of the stable free radical DPPH•

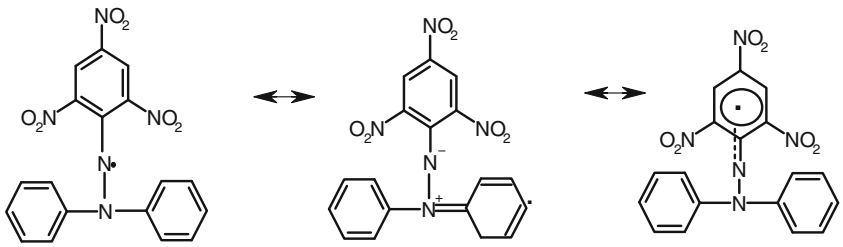

QDs-based fluorescent probes as biosensors for free radicals.

Experimental

Materials

Thioglycolic acid (TGA), $CdCl_2.H_2O$, tellurium powder (200 mesh), Na_2HPO_4, sodium borohydride, 2,2-diphenyl-1-picrylhydrazyl (DPPH•) were obtained from Aldrich. NaCl, methanol, ethanol, and tris (hydroxyl methyl) amino methane were obtained from SAARCHEM. All chemicals were of analytical grade and used without prior purification. All solutions were prepared with ultra pure water of resistivity 18.2 mΩ, obtained from a Milli-Q Water System (Millipore Corp. Bedford, MA, USA). All other reagents were obtained from commercial suppliers and used as received. Tris–HCl Buffer (50 mM) was employed for all studies. The pH was adjusted by addition of 0.1 M NaOH.

Instrumentation

Excitation and emission spectra were recorded on a Varian Eclipse spectrofluorimeter. The excitation wavelength (400 nm) and slit width (each 5 nm) were kept constant for all the experiments. Ground state electronic absorption spectra were recorded on a Shimadzu UV–vis 2550 spectrophotometer in the range 300–800 nm. X-ray powder diffraction patterns were recorded using a Cu kα radiation (λ=1.5405 Å, nickel filter), on a Bruker D8 Discover equipped with a proportional counter. Scanning was at 1° min^{-1} with a filter time-constant of 2.5 s per step and a slit width of 6.0 mm, while data were obtained in the range from 2θ=5° to 60°. A zero background silicon wafer slide was used for sample placement. The X-ray diffraction (XRD) data analysis was carried out using Eva (evaluation curve fitting) software. Subtraction of spline fitted to the curve background was used for baseline correction of each diffraction pattern and the full-width at half maximum values were obtained from the fitted curve. A Metrohm Swiss 827 pH meter was used for pH measurements.

Fluorescence lifetime measurements were carried out using a time correlated single photon counting (TCSPC) setup (FluoTime 200, Picoquant GmbH). The excitation source was a diode laser (LDH-P-C-485 with 10 MHz repetition rate, 88 ps pulse width). Fluorescence was detected under the magic angle with a peltier cooled photomultiplier tube (PMT) (PMA-C 192-N-M, Picoquant) and integrated electronics (PicoHarp 300E, Picoquant GmbH). A monochromator with a spectral width of about 4 nm was used to select the required emission wavelength band. A scattering Ludox solution (DuPont) was used to measure the response function of the system and had a full width at half maximum (FWHM) of about 300 ps. To obtain good statistics, the ratio of stop to start pulses was kept low (below 0.05). Measurement of the entire luminescence decay curve was at the maximum of the emission peak. Data analysis was done using the program Fluofit (Picoquant GmbH). Estimation of the decay error times was carried out using the support plane approach.

Fluorescence Studies

Fluorescence Quantum Yields

Fluorescence quantum yield of the QDs was determined by the comparative method [22].

$$\Phi_F = \Phi_{F(Std)} \frac{F.A_{Std}.n^2}{F_{Std}.A.n^2_{Std}} \quad (1)$$

where A and A_{Std} are the absorbances of the sample and standard at the excitation wavelength, respectively. F and F_{Std} are the areas under the fluorescence curves of the QDs and the standard respectively and n and n_{Std} are the refractive indices of the solvent used for the sample and standard. Rhodamine 6G in ethanol (Φ_F=0.94 [23, 24]) was used as the standard. The excitation wavelength for both the sample and standard was 400 nm and the absorbance was in the range of 0.05 and 0.1.

Fluorescence Quenching Experiments

QDs colloids solution in MeOH:Tris–HCl buffer (30:70) was mixed with known concentrations of DPPH• in the

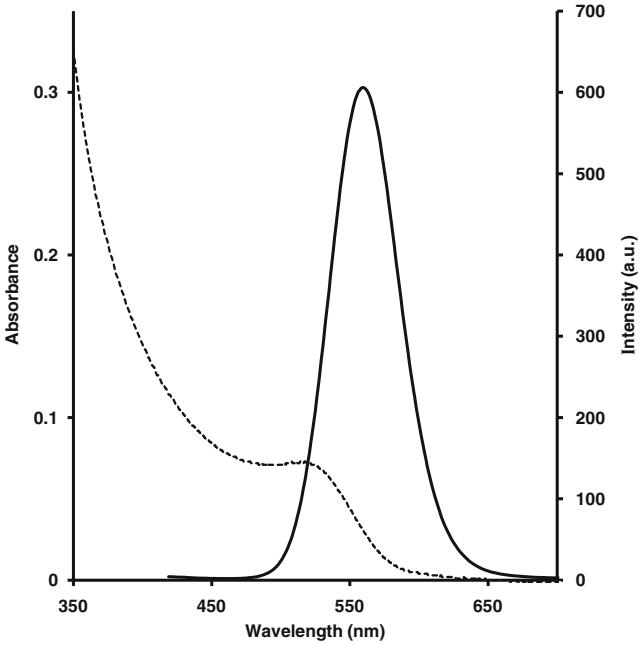

Fig. 1 Absorption (– – –) and fluorescence emission spectra (—) of TGA-capped CdTe QDs at room temperature. λ_{exc}=400 nm. Solvent: 0.1 M NaOH

same solvent mixture. DPPH$^{\bullet}$ has limited solubility in aqueous solution, hence this solvent mixture was employed to improve solubility. The fluorescence spectra of the QDs were recorded under a constant excitation wavelength of 400 nm. The working solutions were stirred vigorously prior to photoluminescence (PL) measurements and all measurements were conducted at room temperature.

Synthesis of TGA Capped CdTe QDs

Synthesis of Sodium Hydrogen Telluride (NaHTe)

The preparation of NaHTe was *via* a method described previously in literature but with some modifications [4]. Briefly, 1.0 mmol of tellurium powder and 2.6 mmol of sodium borohydride (molar ratio of Te to $NaBH_4$ is 1:2.6) were loaded into a 25 ml 3-necked flask and 10 ml of Millipore water was added. The flask was fitted with a septum and the solution deaerated with argon gas at 0 °C. After 8 h, white sodium tetraborate precipitation was formed at the bottom of the flask and the black Te powder fully disappeared, resulting in the formation of the clear supernatant NaHTe which was separated from the solution and used as the Te precursor in the following preparation.

Synthesis and Purification of CdTe QDs

$CdCl_2.H_2O$ and freshly prepared NaHTe were used as precursors for the synthesis of TGA capped QDs *via* a method described previously in literature but with some

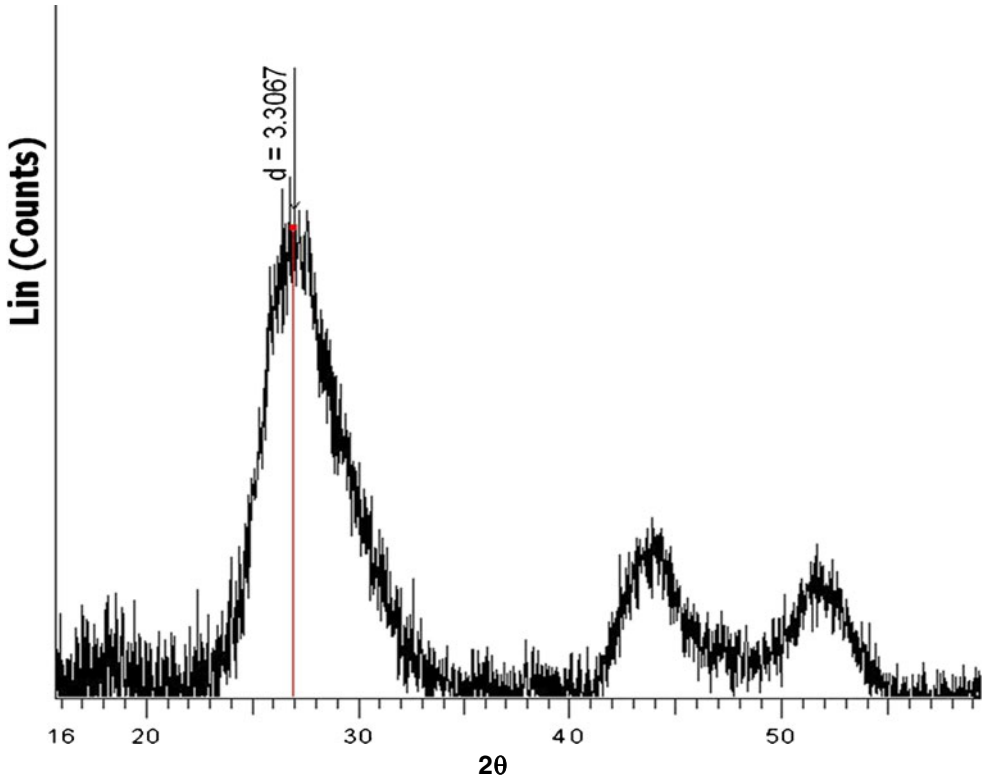

Fig. 2 Powder XRD spectra of the TGA-capped CdTe QDs

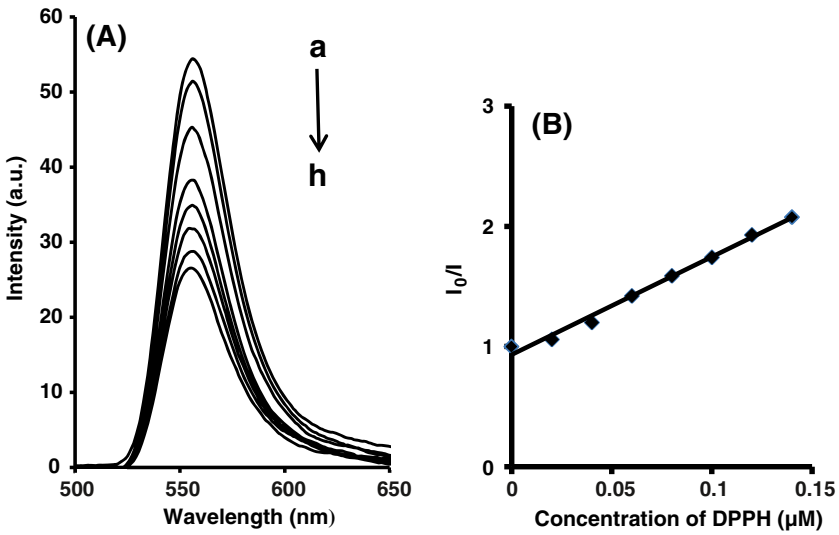

Fig. 3 PL spectra (**A**) of QDs (2.2 nm) in the presence of various concentrations of DPPH$^{\bullet}$ in MeOH:Tris–HCl buffer solution at pH 7.0. *a*: absence of DPPH$^{\bullet}$, *b–h*: 0.02, 0.04, 0.06, 0.08, 0.1, 0.12, 0.14 μM); corresponding Stern-Volmer plot (**B**)

modifications [1]. Briefly, 1 mmol of $CdCl_2.H_2O$ was placed in a 250 ml 3-necked flask attached to a condenser and 110 ml of Millipore water was added, 2.4 mmol of TGA was then injected into the mixture under vigorous stirring. The pH of the solution was adjusted to 11–12 using 0.1 M NaOH and the mixture was deaerated with nitrogen (N_2) gas for 30 min. Freshly prepared oxygen-free NaHTe was then injected into the solution using a syringe and the reaction kept at a constant temperature of 90 °C. In our experiment the molar ratio of Cd^{2+}:NaHTe:TGA was 1:2.6:2.4. To obtain QDs of different sizes, aliquots of the reaction mixture were taken at different time intervals for emission and absorption measurements.

The resulting products were precipitated with ethanol and superfluous of unreacted precursors that did not participate in the reaction were removed via centrifugation at 3,000 rpm for 10 min. The resultant precipitate was re-precipitated with ethanol more than 3 times and dried under vacuum and kept in the dark for further use.

Results and Discussion

Characterization of as Synthesized CdTe QDs

Figure 1, represents typical absorption and photoluminescence (PL) spectra of TGA-capped CdTe QDs taken at room temperature. Two different sizes of QDs with emission peaks at 525 nm and 555 nm were employed in this work. The fluorescence quantum yields (Φ_F) were 0.14 and 0.57 for QDs emitting at 525 nm and 555 nm, respectively. The Φ_F values are known to increase with increase in the size of the QD [25], hence the observed increase in fluorescence quantum yield with emission wavelength.

The sizes of the synthesized CdTe QDs was calculated according to Eq. 2 [26]

$$D = \left(9.8127 \times 10^{-7}\right)\lambda^3 - \left(1.7147 \times 10^{-3}\right)\lambda^2 + (1.0064)\lambda - (194.84) \quad (2)$$

where λ is the absorption maxima of the QDs.

The sizes of QDs obtained in our study were calculated to be 2.1 nm and 3.0 nm for QDs with emission peaks at 525 and 555 nm, respectively. The fitting function (Eq. 2) is not valid for QDs of sizes outside the range 1–9 nm [27].

X-ray powder diffraction can provide useful information about the crystal structure and size of CdTe QDs. Figure 2 represents the X-ray diffraction pattern obtained from powdered precipitated fractions of TGA-capped CdTe QDs used in this work. Peaks occur at 27.1°, 44.0° and 51.6°. The sizes of the QDs were also

Table 1 Static quenching rate constants (K_S) calculated from the fluorescence data of TGA-capped QD-DPPH$^{\bullet}$ system at pH 4.8, pH 7.0 and pH 10.3 respectively

QD size (nm)	pH	K_S (10^6 M^{-1})
2.2	4.8	8.43
	7.0	8.03
	10.3	6.71
2.6	4.8	7.41
	7.0	7.32
	10.3	7.29

determined using XRD, according to the Scherrer equation. (Eq. 3).

$$d(\text{Å}) = \frac{k\lambda}{\beta Cos\theta} \quad (3)$$

where λ is the wavelength of the X-ray source (1.5405), k is an empirical constant equal to 0.9, β is the full width at half maximum of the diffraction peak, and θ is the angular position. TGA-capped CdTe QDs obtained from XRD calculation are 2.2 and 2.6 nm, which are similar to those from the polynomial (Eq. 2), although the latter is just an estimation. XRD sizes will be employed in this work.

Quenching of Fluorescence of TGA-Capped CdTe QDs by DPPH•

Factors such as pH values, electron donors/acceptors, and ionic strength have been reported to have great influence on

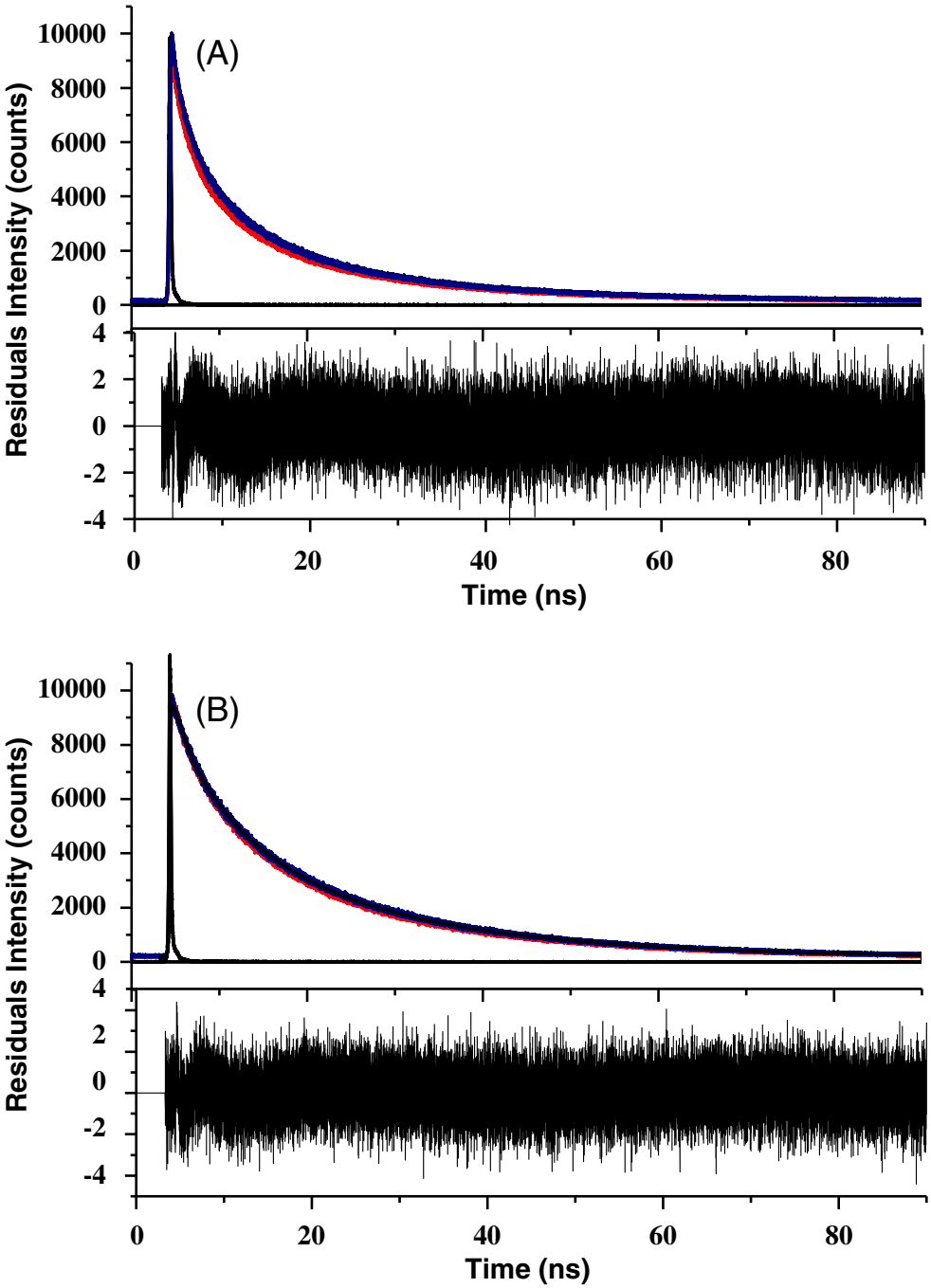

Fig. 4 Fluorescence decay curves of 2.2 nm CdTe QDs (**A**) and 2.6 nm CdTe QDs (**B**) in the absence (*red*) and presence (*blue*) of 0.04 μM DPPH• in MeOH:Tris–HCl buffer solutions at pH 7.0 respectively

the PL emission spectra of QDs. The influence of pH has been reported [1, 28, 29] hence the quenching of QDs emission by DPPH$^{\bullet}$ was recorded at different pHs (4.8, 7.0 and 10.3). Figure 3 shows the quenching of 2.2 nm QDs emission on addition of various amounts of DPPH$^{\bullet}$ recorded at pH 7.0 (as a representative of the rest of the pHs). The PL intensity decreased gradually with increasing concentration of DPPH$^{\bullet}$. No visible changes in the shape of the fluorescence spectra were observed upon quenching. The quenching of QDs fluorescence by DPPH$^{\bullet}$, may be represented by the Stern-Volmer equation (Eq. 4).

$$\frac{I_0}{I} = 1 + K_s(Q) \tag{4}$$

where I_0 and I are the steady-state PL intensity in the absence and presence of the quencher (DPPH$^{\bullet}$); K_S is the static quenching rate constant and [Q] is the concentration of quencher (DPPH$^{\bullet}$). As shown in Fig. 3, linear Stern-Volmer plots were obtained for all pH conditions (pH 4.8, 7.0, and 10.3) irrespective of the QDs size.

Table 1, lists the K_S values for both 2.2 nm and 2.6 nm QDs. From the high values of K_S at low pH, it can be concluded that the QDs are more exposed to quenching than at low pH. As reported before [30], the change of pH influences the surface of the QDs. At low pH levels, capping agents may be removed from the surface of the QDs; hence exposing the QDs to more quenching and hence larger K_S values. At high pH, the instability of DPPH$^{\bullet}$ has been proposed [21]. This may suggest the lower quenching efficiency observed in alkaline media in addition to pH effects on QDs. Whether a linear or curved (upward or downward) Stern-Volmer plot is obtained for static quenching depends on the association constants [31], thus linear plots may be obtained for static quenching.

Fluorescence lifetime measurements are the most useful method for differentiating between static and dynamic quenching [32]. Figure 4 shows the fluorescence decay curves of CdTe QDs in the absence and presence of DPPH$^{\bullet}$. The QDs exhibit triexponential decay in the presence and absence of DPPH$^{\bullet}$ and the lifetimes are listed in Table 2. The longer lifetime τ_1, is associated with

Table 2 Fluorescence lifetime of TGA-capped CdTe QDs in the absence and presence of DPPH$^{\bullet}$

QD (nm)	[DPPH$^{\bullet}$] (μM)	τ_2 (ns) [a] (±0.15)	τ_2 (ns) [a] (±0.09)	τ_3 (ns) [a] (±0.01)	Mean lifetimes (ns) (±0.1)
2.2	0	20.1 (0.66)	6.1 (0.30)	0.9 (0.04)	9.0
	0.02	20.6 (0.67)	6.3 (0.28)	1.0 (0.05)	9.3
	0.04	20.4 (0.67)	6.3 (0.29)	1.0 (0.04)	9.2
	0.06	20.2 (0.67)	6.2 (0.29)	0.9 (0.04)	9.1
2.6	0	22.5 (0.75)	7.8 (0.23)	1.1 (0.02)	10.5
	0.02	22.4 (0.77)	7.8 (0.21)	1.1 (0.02)	10.5
	0.04	22.6 (0.77)	7.9 (0.21)	1.1 (0.02)	10.5
	0.06	22.4 (0.77)	7.7 (0.21)	1.0 (0.02)	10.4

[a] Relative abundance in brackets

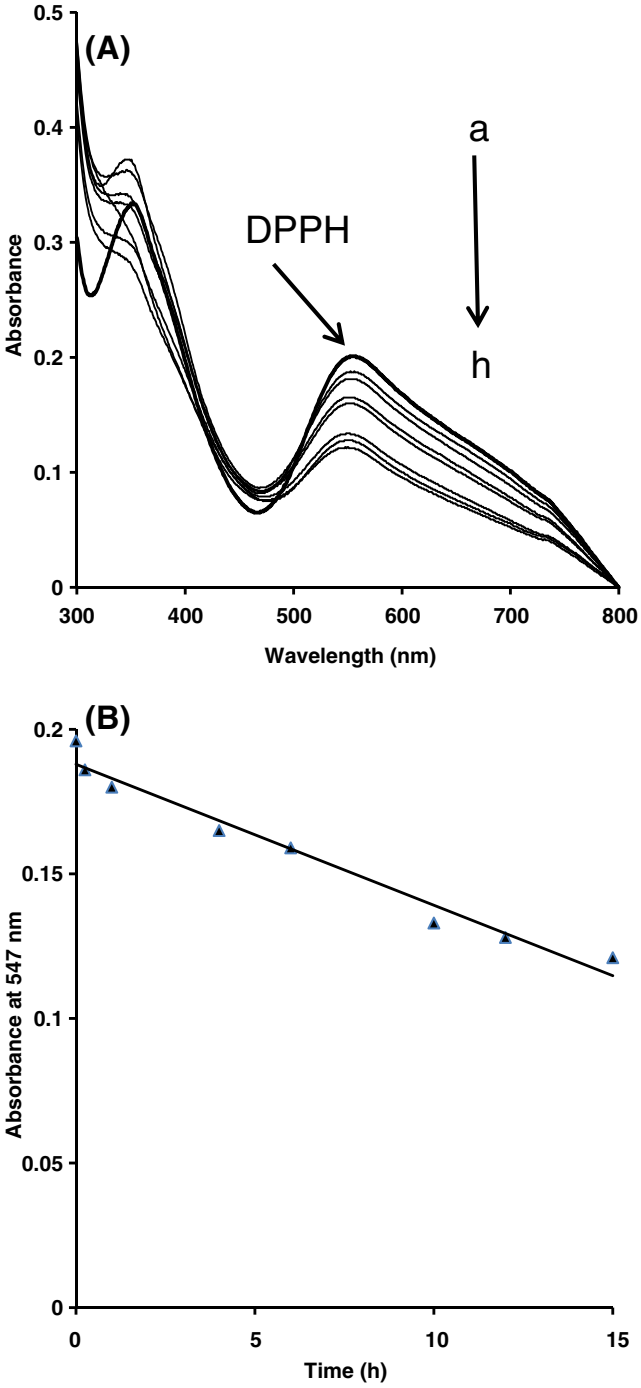

Fig. 5 **A** UV–vis absorption spectral changes observed following addition of 2.2 nm QDs (1.8 μM) to solutions of 0.1 μM DPPH$^{\bullet}$; *a*: absence of QDs, *b-h* (DPPH$^{\bullet}$+QDs): 0.25, 1, 4, 6, 10, 12, 15 h). **B** Corresponding plot of absorbance maximum at 547 nm against time for DPPH$^{\bullet}$. Solvent: MeOH:Tris–HCl buffer solution (pH 7.0)

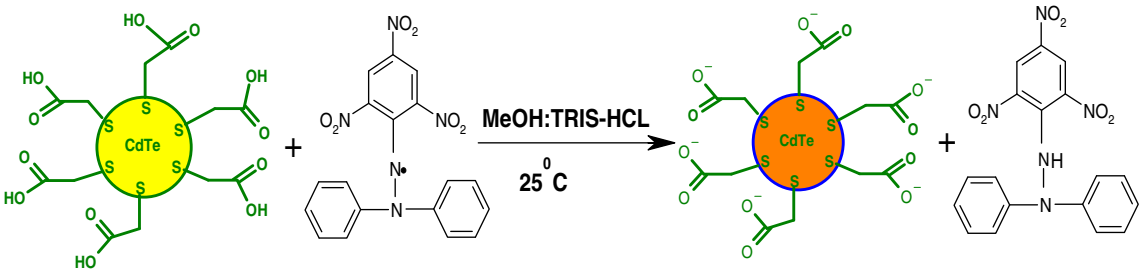

Scheme 2 Proposed reaction between DPPH• with CdTe QDs

the involvement of surface states in the carrier recombination process [33], the intermediate lifetime τ_2 could be as a result of intrinsic recombination of initially populated core states [34] while the shortest lifetime τ_3 is associated with radiative depopulation due to band edge recombination at the surface [34–37]. No changes were observed in the fluorescence lifetimes in the absence and presence of DPPH• and when increasing the concentration of DPPH•, Table 2. For dynamic quenching, the fluorescence lifetimes vary proportionally with the quencher concentration while in the case of static quenching, the lifetimes are independent of quencher concentration [33, 37]. The fact that the fluorescence lifetime values are virtually constant in Table 2, suggests that static quenching predominates.

Kinetics of the Interaction of DPPH• with TGA-Capped CdTe

There have been very few reports on the antioxidant activity and the catalytic ability of inorganic nanoparticles to scavenge free radicals [38–40]. To further understand the interaction between CdTe QDs and DPPH•, we have investigated the interaction of TGA-capped CdTe QDs with DPPH• free radicals. Figure 5 presents UV–vis absorption spectral changes (with time) of DPPH• in the presence of CdTe QDs. On addition of QDs to DPPH•, there was evidence of enhancement of the absorption peaks due to DPPH• at wavelengths shorter than 400 nm, Fig. 5. The DPPH• peak at 350 nm is enhanced and also shifts with time confirming formation of a new product between DPPH• and QDs. This observation suggests static quenching. It could be seen that the absorption maximum at 547 nm due to DPPH•, decreased with time at a fixed concentration of the QDs. However, the decrease in absorbance was slow and strongly dependent on the nanoparticle size with the purple colour of the radical being bleached gradually. Notwithstanding, the decrease in absorbance was detectable within 15 min of the reaction and confirms an efficient scavenging of DPPH• and a possible reduction to 2,2-diphenyl-1-picrylhydrazine (DPPH-H), Scheme 2, at pH 7.

Kinetics of the CdTe QDs-DPPH system follow a first-order-reaction as shown in Fig. 5b. The first-order reaction rate constants (k) were evaluated from the slope of each line and are: 0.30 min^{-1} for 2.2 nm QDs and 0.22 min^{-1} for 2.6 nm QDs respectively, at pH 7.0. Thus the smaller QDs react with DPPH• faster than the larger ones. Since thioglycolic acid (used as capping agent) is also a known reducing agent [41], experiments were performed where the capping agent (TGA) alone was added to DPPH•, and spectral changes similar to those in Fig. 5 were observed. Thus the changes in the rate constants are related to the number of TGA capping agents which would be more for the smaller QDs, hence the larger rate constant compared with the larger QDs.

Conclusions

In this study, the interaction between TGA-capped CdTe QDs and DPPH• free radical has been studied by UV-visible absorption and by steady state and time resolved fluorescence measurements. The results show clearly that DPPH• effectively quenches the fluorescence of TGA-capped CdTe QDs through formation of a ground state complex (static quenching) which was confirmed by fluorescence lifetime studies. The quenching behaviour was described by the Stern-Volmer relationship and a linear relationship was observed. Time course absorption studies revealed that DPPH• could be reduced to its subsequent hydrazine form, DPPH-H in the presence of CdTe QDs. The fact that QDs showed efficient fluorescent quenching sensitivity towards DPPH radical investigated indicates that they hold promising application for development of probes as sensors for detection of organic free radicals.

Acknowledgements This work was supported by the Department of Science and Technology (DST) and National Research Foundation (NRF), South Africa through DST/NRF South African Research Chairs Initiative for Professor of Medicinal Chemistry and Nanotechnology as well as Rhodes University and DST/Mintek Nanotechnology Innovation Centre (NIC) – Sensors, South Africa.

References

1. Yun-Sheng X, Chang-Qing Z (2009) Interaction of CdTe nanocrystals with thiol-containing amino acids at different pH: a fluorimetric study. Microchim Acta 164:29–34
2. Ming H, Jia N (2010) Determination of vanadium (V) with CdTe quantum dots as fluorescent probes. Anal Bioanal Chem 397:3589–3593
3. Ling D, Zhou PJ, Li SQ, Shi GY, Zhong T, Wu M (2011) Spectroscopic studies on the thermodynamic of L-cysteine capped CdSe/CdS quantum dots-BSA interaction. J Fluoresc 21:17–24
4. Fan J, Zhou J, Sun T, Lu S, Tang J, Lu J (2010) Multi-spectroscopic study on the interaction between CdTe quantum dots and bovine serum albumin. Chin J Chem 28:2353–2358
5. Juan-Juan P, Shao-Pu L, Lei W, You-Qiu H (2010) Studying the interaction between CdTe quantum dots and nile blue by absorption, fluorescence and resonance rayleigh scattering spectra. Spectrochimica Part A 75:1571–1576
6. Raquel EG, Miguel-De-La G (2009) The use of quantum dots in organic chemistry. Trends Anal Chem 28:279–291
7. Ken-Tye Y, Wing-Cheung L, Indrajit R, Zhu J, Huijie H, Mark TS, Paras NP (2011) Aqueous phase synthesis of CdTe quantum dots for biophotonics. J Biophotonics 4:9–20
8. Xianxiang W, Yi L, Xiandeng H (2011) A potential visual fluorescence probe for ultratrace arsenic (III) detection by using glutathione-capped CdTe quantum dots. Talanta 84:382–386
9. Victor IK (2010) Nancrystal quantum dots. CRC, Florida
10. Mulder WJM, Koole R, Brandwijk RJ, Storm G, Chin PTK, Strijkers GJ, De-Donega C, Nicolay K, Griffioen AW (2006) Quantum dots with a paramagnetic coating as a bimodal molecular imaging probe. Nano Lett 6:1–6
11. Jin WJ, Fernandez-Arguelles MT, Costa-Fernandez JM, Pereiro R, Sanz-Medel A (2005) Photoactivated luminescent CdSe quantum dots as sensitive cyanide probes in aqueous soultions. Chem Commun 883–885
12. Tomasulo M, Yildiz I, Raymo FM (2006) pH-sensitive quantum dots. J Phys Chem B 110:3853–3855
13. Ping Z, Ying Y, Jianzhong W, Yan L, Bo C, Zhaoyang L, Chunsui L (2006) Preparation and application of functionalized nanoparticles of CdSe capped with 11-mercaptoundecanoic acid as a fluorescent probe. Talanta 70:902–906
14. Qiao X, Jian-Hao W, Zhan W, Zhao-Hui Y, Qin Y, Yuan-Di Z (2008) Interaction of CdTe quantum dots with DNA. Electrochem Commun 10:1337–1339
15. Callen JF, Mulrooney RC, Sukanta K, Bridgeen M (2008) Anion sensing with luminescent quantum dots – a modular approach based on the photoinduced electron transfer (PET) mechanism. J Fluoresc 18:527–532
16. Neuman D, Ostrowski AD, Mikhailovsky AA, Absalonson RO, Strouse GF, Ford PC (2008) Quantum dot fluoresence quenching pathways with Cr (III) complexes. Photosensitized NO Production from trans-Cr(cyclam)$(ONO)_2^+$. J Am Chem Soc 130:168–175
17. Jin T, Fujii F, Yamada E, Nodasaka Y, Kinjo M (2007) Preparation and characterization of thiacalix[4]arene coated water-soluble CdSe/ZnS quantum dots as a fluorescent probe for Cu^{2+} ions. Comb Chem High Throughput Screening 10:473–479
18. Vincent M, Marie L, Paul B, Robert G, Scaiano JC (2006) Free radical sensor based on CdSe quantum dots with added 4-Amino-2,2,6,6-Tetramethylpiperidine oxide functionality. J Phys Chem B 110:16353–16358
19. Jie FS, Cui LR, Li HL, Xing GC (2008) CdTe quantum dots as fluorescence sensor for the determination of vitamin B6 in aqueous solution. Chin Chem Lett 19:855–859
20. Wenfeng Z, Yingsing F, Waisum O, Cheung MPL (2010) L-cysteine-capped CdTe quantum dots as fluoresencence probe for determination of cardiolipin. Anal Sci 26:879–884
21. Ionita P (2005) Is DPPH stable free radical a good scavenger for oxygen active species? Chem Pap 59:11–16
22. Fery-Forgues S, Lavabre D (1999) Are fluorescence quantum yields so tricky to measure? A demonstration using familiar stationery products. J Chem Ed 76:1260–1264
23. Lakowicz JR (1999) Principles of fluorescence spectroscopy. Plenum, New York
24. Hao Z, Zhen Z, Bai Y (2003) The influence of carboxyl groups on the photoluminescence of mercaptocarboxylic acid-stabilized CdTe nanoparticle. J Phys Chem B 107:8–13
25. Idowu M, Chen J-Y, Nyokong T (2008) Photoinduced energy transfer between water-soluble CdTe quantum dots and aluminium tetrasulfonated phthalocyanine. New J Chem 32:290–296
26. Yu WW, Qu L, Guo W, Peng X (2003) Experimental determination of the extinction coefficient of CdTe, CdSe, and CdS nanocrystals. Chem Mater 15:2854–2860
27. Guo W, Li JJ, Wang YA, Peng X (2003) Luminescent CdSe/CdS core/shell nanocrystals in dendron boxes: superior chemical, photochemical and thermal stability. J Am Chem Soc 125:3901–3909
28. Jipei Y, Weiwei G, Erkang W (2008) Investigation of some critical parameters of buffer conditions for the development of quantum dots-based optical sensors. Anal Chim Acta 630:174–180
29. Duyang G, Zonghai S, Heyou H (2010) A novel method for the analysis of calf thymus DNA based on CdTe quantum dots-Ru$(bpy)_3^{2+}$ photoinduced electron transfer system. Microchim Acta 168:341–345
30. Mandal A, Tamai N (2008) Influence of acid on luminescence properties of thioglygolic acid-capped CdTe quantum dots. J Phys Chem C 112:8244–8250
31. Blatt E, Mau AWH, Sasse WHF, Sawyer WH (2008) Simulated Stern-Volmer Plots for 1–1 Ground-State Complexation. Aust J Chem 41:127–131
32. Jhonsi MA, Renganathan R (2010) Investigation on the photoinduced interaction of water soluble thioglycolic acid (TGA) capped CdTe quantum dots with certain porphyrins. J Colloid Interface Sci 344:596–602
33. Wang X, Qu L, Zhang J, Peng X, Xiao M (2003) Surface-related emission in highly luminescent CdSe quantum dots. Nano Lett 3:1103–1106
34. Sanz M, Correa-Duarte MA, Liz-Marzan LM, Douhal A (2008) Femtosecond dynamics of CdTe quantum dots in water. J Photochem Photobiol A: Chem 196:51
35. Chong EZ, Matthews DR, Summers HD, Njoh KL, Errington RJ, SmithPJ (2007) Development of fret-based assays in the far-red using CdTe quantum dots. J Biomed Biotechnol 54169
36. Javier A, Magana D, Jennings T, Strouse GF (2003) Nanosecond exciton recombination dynamics in colloidal CdSe quantum dots under ambient conditions. Appl Phys Lett 83:1423–1425
37. Zhang JY, Wang XY, Xiao M (2002) Modification of spontaneous emission of CdSe/CDS quantum dots in the presence of a semiconductor interface. Opt Lett 27:1253–1255
38. Geckeler KE, Samal S (2001) Rapid assessment of the free radical scavenging property of fullerenes. Fullerene Sci Technol 9:17–23
39. Paul S, Saikia JP, Samdarshi SK, Konwar BK (2009) Investigation of antioxidant property of iron oxide particles by 1,1-diphenylpicrylhydrazyle (DPPH) method. J Magn Magn Mater 321:3621–3623
40. Ryoko I, Tomokazu Y, Kunio E (2005) Preparation of Au/TiO_2 nanocomposites and their catalytic activity for DPPH radical scavenging reaction. J Colloid Interface Sci 288:177–183
41. Demirhan F, Taban G, Baya M, Dinoi C, Daran J-C, Poli R (2006) Reduction of $[Cp_2^*Mo_2O_5]$by thioglycolic acid in an aqueous medium: Synthesis and structure of $[\{Cp^*Mo(\mu\text{-}SCH_2COO)\}_2(\mu\text{-}S)]$. J Organomet Chem 691:648–654